Membrane Matrix for the Hydrolysis of Amino Acid Esters with Marked Enantioselectivity†[1]

Ryuichi Ueoka,*[2a] Yōko Matsumoto,[2a] Robert A. Moss,*[2b] Shanti Swarup,[2b] Atsushi Sugii,[2c] Kumiko Harada,[2c] Jun-ichi Kikuchi,[2d] and Yukito Murakami*[2d]

Contribution from the Department of Industrial Chemistry, Kumamoto Institute of Technology, Kumamoto 860, Japan, The Wright and Rieman Laboratories, Department of Chemistry, Rutgers, The State University of New Jersey, New Brunswick, New Jersey 08903, Faculty of Pharmaceutical Sciences, Kumamoto University, Kumamoto 862, Japan, and Department of Organic Synthesis, Faculty of Engineering, Kyushu University, Fukuoka 812, Japan.
Received June 10, 1987

Abstract: The stereoselective hydrolysis of the long-chain substrate (*p*-nitrophenyl *n*-dodecanoyl-D(L)-phenylalanininate, D(L)-S_{12}) in surfactant aggregates has been found to be easily controlled by changing the reaction temperature, amino acid sequence in peptide catalysts, and composition of the aggregates. First, the stereoselectivity (reflected in $k^{L}_{a,obsd}/k^{D}_{a,obsd}$) for the hydrolysis of S_{12} in the catalytic system of *N*-tetradecanoyl-L-histidyl-L-leucine (MyrHisLeu) and dialkyldimethylammonium bromide ($2C_nBr$; n = 14, 16) was elevated at temperatures somewhat higher than the aggregate phase transitions. Interestingly, the optimum temperature (25 °C) for enantioselectivity in the $2C_{14}Br$ vesicular system was in fair agreement with the inflection point (25 °C) in the polarization–temperature dependence of 1,6-diphenyl-1,3,5-hexatriene as a probe in the hydrophobic region of the vesicles. These results suggest that the hydrophobic microenvironment of the membrane matrix ($2C_nBr$) changes at the optimum temperature for the great enhancement of stereoselectivity. Second, the LLL-tripeptide *N*-(benzyloxycarbonyl)-L-phenylalanyl-L-histidyl-L-leucine (Z-PheHisLeu) was most efficient for the enhancement of enantioselectivity (affording $k^{L}_{a,obsd}/k^{D}_{a,obsd}$ = 27) among all the peptide catalysts in this study. Furthermore, a large enhanced enantioselectivity was obtained for the hydrolysis of S_{12} with Z-PheHisLeu in a coaggregate system, which was composed of the double- and single-chain cationic surfactants. Especially noteworthy is the fact that the high enantioselectivity ($k^{L}_{a,obsd}/k^{D}_{a,obsd}$ = 27) of S_{12} with Z-PheHisLeu in the vesicular system of $2C_{14}Br$ (1 mM) was elevated dramatically by the addition of hexadecyltrimethylammonium bromide (CTAB) and reached the enantiomer rate constant ratio ($k^{L}_{a,obsd}/k^{D}_{a,obsd}$) = 71 at 25 °C in coaggregates of 33 mol % $2C_{14}Br$/67 mol % CTAB. These coaggregates appear to be large and rodlike particles with diameters of 600–1600 Å from electron microscopic and dynamic light-scattering results. Finally, with respect to the origin of enantioselectivity, it is emphasized on the basis of circular dichroism experiments that the fitting of the L isomer substrate (L-S_{12}) and the active tripeptide (Z-PheHisLeu) having a hydrophobic pocket through the intramolecular interactions of amino acid residues should be extremely important to enhance the enantioselectivity and, subsequently, the adjusting of the hydrophobic microenvironment to the optimum fit of reactants by changing the composition of coaggregates would induce the highest enantioselectivity.

The stereoselective hydrolysis of N-protected amino acid esters has recently attracted considerable attention in connection with understanding the origins of the stereoselectivity observed with proteolytic enzymes. Very recently, many interesting results have been obtained in the micellar,[3] vesicular,[4] cyclic peptide,[5] and macromolecular systems.[6]

In the course of our study on enantioselective micellar catalysis, the following interesting kinetic results were obtained.[3a,7] (i) The hydrophobicity of enantiomeric substrates and L-histidine derivatives plays an important role in enhancing both the catalytic activity and enantioselectivity in cationic micellar systems. (ii) The cooperative interaction of chiral nucleophiles (L-histidine derivatives) with chiral surfactants very efficiently enhances the enantioselectivity toward enantiomeric substrates. (iii) The binding constants for all the L isomer substrates are generally smaller than those for the corresponding D isomers, even though the reaction rates for the L isomers are much greater than those for the corresponding D isomers. Furthermore, noteworthy aspects in the vesicular systems are as follows. (iv) Bilayer systems in the liquid-crystalline state give rise to greater hydrolysis rates and stereoselectivities compared with those in the gel state, even though differences in binding properties between L and D isomers were not observed in both states.[4b] (v) The bilayer (liquid-crystalline) catalytic systems tend to be governed by the entropy of activation in relation to the isokinetic temperature (β), and this is different from the enthalpy-driven micellar systems.[4d,7d] (vi) The enantioselectivity is markedly improved at temperatures somewhat higher than the phase transitions.[1a] (vii) Addition of single-chain surfactants[4d] or cholesterol[9] to the bilayer catalytic systems alters the hydrophobicity of the membrane matrix and results in very high enantioselectivity for the hydrolysis of long-chained enantiomeric substrates. Most recently, the authors have found appropriate systems to control the stereoselectivity of hydrolysis. That is, the enantioselectivity for the cleavage of the long-chained substrates (**1b**, D(L)-S_{12}) by the tripeptide catalyst (**6**, Z-PheHisLeu) was well correlated with the apparent mean hydrody-

† Dedicated to the memory of Professor Iwao Tabushi.

(1) Preliminary communications: (a) Ueoka, R.; Matsumoto, Y.; Nagamatsu, T.; Hirohata, S. *Chem. Lett.* **1984**, 583. (b) Ueoka, R.; Matsumoto, Y.; Ihara, Y. *Ibid.* **1984**, 1807. (c) Ueoka, R.; Moss, R. A.; Swarup, S.; Matsumoto, Y.; Strauss, G.; Murakami, Y. *J. Am. Chem. Soc.* **1985**, *107*, 2185. (d) Ueoka, R.; Matsumoto, Y.; Yoshino, T.; Hirose, T.; Moss, R. A.; Kim, K. Y.; Swarup, S. *Tetrahedron Lett.* **1986**, 1183.

(2) (a) Kumamoto Institute of Technology. (b) Rutgers University. (c) Kumamoto University. (d) Kyushu University.

(3) (a) Ueoka R.; Murakami, Y. *J. Chem. Soc., Perkin Trans. 2* **1983**, 219. (b) Ihara, Y.; Hosako, R.; Nango, M.; Kuroki, N. *Ibid.* **1983**, 5. (c) Moss, R. A.; Lee, Y.-S.; Lukas, T. J. *J. Am. Chem. Soc.* **1979**, *101*, 2499. (d) Ihara, Y.; Kunikiyo, N.; Kunimasa, T.; Kimura, Y.; Nango, M.; Kuroki, N. *J. Chem. Soc., Perkin Trans. 2* **1983**, 1741. Z-LeuHis and Z-PheHis were provided by courtesy of Prof. Y. Ihara of Yamaguchi Women's University.

(4) (a) Murakami, Y.; Nakano, A.; Yoshimatsu, A.; Fukuya, K. *J. Am. Chem. Soc.* **1981**, *103*, 728. (b) Ueoka, R.; Matsumoto, Y.; Ninomiya, Y.; Nakagawa, Y.; Inoue, K.; Ohkubo, K. *Chem. Lett.* **1981**, 785. (c) Moss, R. A.; Taguchi, T.; Bizzigotti, G. O. *Tetrahedron Lett.* **1982**, 1985. (d) Ueoka, R.; Matsumoto, Y.; Nagamatus, T.; Hirohata, S. *Tetrahedron Lett.* **1984**, 1363.

(5) (a) Kawaguchi, K.; Tanihara, M.; Imanishi, Y. *Polym. J. (Tokyo)* **1983**, *15*, 97. (b) Tanihara, M.; Imanishi, Y. *Ibid.* **1983**, *15*, 499.

(6) (a) Kimura, Y.; Nango, M.; Ihara, Y.; Kuroki, N. *Chem. Lett.* **1984**, 429. (b) Kimura, Y.; Kanda, S.; Nango, M.; Ihara, Y.; Koga, J.; Kuroki, N. *Ibid.* **1984**, 433.

(7) (a) Ueoka, R.; Terao, T.; Ohkubo, K. *Nippon Kagagu Kaishi*, **1980**, 462. (b) Ohkubo, K.; Sugahara, K.; Yoshinaga, K.; Ueoka, R. *J. Chem. Soc., Chem. Commun.* **1980**, 637. (c) Ohkubo, K.; Sugahara, K.; Ohta, H.; Tokuda, K.; Ueoka, R. *Bull. Chem. Soc. Jpn.* **1981**, *54*, 576. (d) Matsumoto, Y.; Ueoka, R. *Bull. Chem. Soc. Jpn.* **1983**, *56*, 3370.

(8) (a) Ueoka, R.; Muramatsu, H. *J. Mol. Catal.* **1982**, *14*, 253. (b) Ueoka, R.; Matsumoto, Y.; Kikuno, T.; Okada, K. *Ibid.* **1983**, *18*, 267.

(9) Ueoka, R.; Matsumoto, Y. *J. Org. Chem.* **1984**, *49*, 3774.

0002-7863/88/1510-1588$01.50/0

namic diameter (d_{hy}) of coaggregates that were composed of a double-chained surfactant and a single-chained one.[1c]

In order to examine the kinetic origin of this enantioselectivity, we investigated in the present work the hydrolytic cleavage of *p*-nitrophenyl *N*-acyl-D(L)-phenylalaninates (D(L)-S_2 (**1a**), D(L)-S_{12} (**1b**)) and *N*-(benzyloxycarbonyl)-D(L)-phenylalaninates (D(L)-ZS (**1c**)) catalyzed by L-histidine derivatives (Z-His (**2a**), MyrHis (**2b**), Z-HisLeu (**3a**), MyrHisLeu (**3b**), Z-HisPhe (**3c**), Z-LeuHis (**4a**), Z-PheHis (**4b**), Bz-GlyHisLeu (**5**), Z-PheHisLeu (**6**)) in vesicular ($2C_{14}Br$ (**7a**), $2C_{16}Br$ (**7b**), $2C_{16}Cl$ (**7c**)), micellar (CTAB (**8a**), CTA-Cl (**8b**)), and coaggregate systems of the double-chain ($2C_{14}Br$, $2C_{16}Cl$) and single-chain (CTAB, CTA -Cl) surfactants.

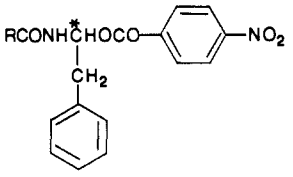

1a: R = CH_3 (D(L)-S_2)
b: R = $CH_3(CH_2)_{10}$ (D(L)-S_{12})
c: R = $PhCH_2O$ (D(L)-ZS)

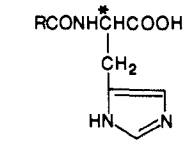

2a: R = $PhCH_2O$ (Z-His)
b: R = $CH_3(CH_2)_{12}$ (MyrHis)

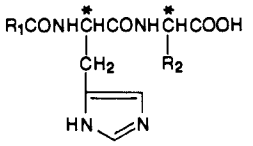

3a: R_1 = $PhCH_2O$, R_2 = $(CH_3)_2CHCH_2$ (Z-HisLeu)
b. R_1 = $CH_3(CH_2)_{12}$, R_2 = $(CH_3)_2CHCH_2$ (MyrHisLeu)
c: R_1 = $PhCH_2O$, R_2 = $PhCH_2$ (Z-HisPhe)

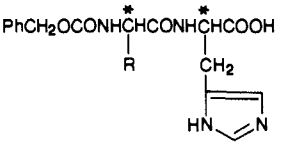

4a: R = $(CH_3)_2CHCH_2$ (Z-LeuHis)
b: R = $PhCH_2$ (Z-PheHis)

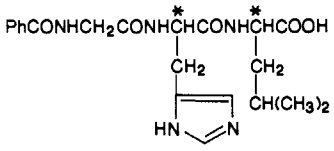

5 (Bz-GlyHisLeu)

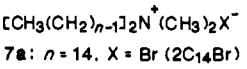

7a: *n* = 14, X = Br ($2C_{14}Br$)
b: *n* = 16, X = Br ($2C_{16}Br$)
c: *n* = 16, X = Cl ($2C_{16}Cl$)

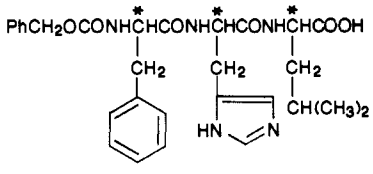

6 (Z-PheHisLeu)

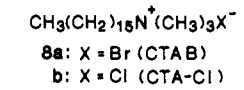

8a: X = Br (CTAB)
b: X = Cl (CTA-Cl)

Furthermore, the relationships between the stereoselectivity and the morphology of the aggregates on the basis of light-scattering and electron miroscopic measurements and the conformation of active tripeptide (Z-PheHisLeu) on the basis of circular dichroism (CD) measurements are discussed.

Experimental Section

Materials. ***p*-Nitrophenyl *N*-Acetyl-D(L)-phenylalaninate** (D(L)-S_2 (**1a**)) **and *p*-Nitrophenyl *N*-Dodecanoyl-D(L)-phenylalaninate** (D(L)-S_{12} (**1b**)). The enantiomeric substrates (D(L)-**1a**, **b**) were prepared from *N*-(benzyloxycarbonyl)-D(L)-phenylalaninate by the esterification of the COOH group with *p*-nitrophenol and dicyclohexylcarbodiimide,[10] followed by hydrobromination of the NH_2 group,[11] and then acylation of the NH_2·HBr group with acetic anhydride or dodecanoic anhydride.[10] Satisfactory results of elemental analyses and specific rotations were obtained for D(L)-**1a** and D(L)-**1b**. D-**1a**: mp 133.5–134.0 °C (lit.[11] mp 135–137 °C); $[\alpha]^{25}_D$ +18.15° (*c* 2, $CHCl_3$) (lit.[11] $[\alpha]^{20}_D$ +17.4° (*c* 2, $CHCl_3$)). Anal. Calcd for $C_{17}H_{16}N_2O_5$: C, 62.19; H, 4.91; N, 8.55. Found: C, 62.08; H, 4.83; N, 8.49. L-**1a**: mp 137.5–138 °C (lit.[11] mp 140–140.5 °C); $[\alpha]^{25}_D$ −17.57° (*c* 2, $CHCl_3$) (lit.[11] $[\alpha]^{20}_D$ −18.6° (*c* 2, $CHCl_3$)). Anal. Found: C, 62.08; H, 4.80; N, 8.48. D-**1b**: mp 108.0–108.2 °C; $[\alpha]^{23}_D$ +10.8° (*c* 2, $CHCl_3$). Anal. Calcd for $C_{27}H_{36}N_2O_5$: C, 69.21; H, 7.74; N, 5.98. Found: C, 69.32; H, 7.94; N, 5.98. L-**1b**: mp 107.0–107.5 °C; $[\alpha]^{23}_D$ −10.8° (*c* 2, CH_3Cl). Anal. Found: C, 69.15; H, 7.76; N, 5.91.

***p*-Nitrophenyl *N*-(Benzyloxycarbonyl)-D(L)-phenylalaninate** (D(L)-**ZS** (**1c**)). The enantiomeric substrates (D(L)-**1c**) were prepared from *N*-(benzyloxycarbonyl)-D(L)-phenylalaninate by the esterification of the COOH group with *p*-nitrophenol and dicyclohexylcarbodiimide.[10] Satisfactory elemental analyses were obtained for D(L)-**1c**. D-**1c**: mp 121.5–123.5 °C (lit.[10] mp 126–126.5 °C). Anal. Calcd for $C_{23}H_{20}N_2O_6$: C, 65.70; H, 4.78; N, 6.66. Found: C, 65.88; H, 4.70; N, 6.67. L-**1c**: mp 119–120 °C (lit.[10] mp 126–126.5 °C). Anal. Found: C, 65.65; H, 4.73; N, 6.59.

***N*-(Benzyloxycarbonyl)-L-histidine** (**Z-His** (**2a**)), ***N*-(Benzyloxycarbonyl)-L-histidyl-L-leucine** (**Z-HisLeu** (**3a**)), ***N*-(Benzyloxycarbonyl)-L-histidyl-L-phenylalanine** (**Z-HisPhe** (**3c**)), ***N*-(Benzyloxycarbonyl)-L-leucyl-L-histidine** (**Z-LeuHis** (**4a**)), ***N*-(Benzyloxycarbonyl)-L-phenylalanyl-L-histidine** (**Z-PheHis** (**4b**)), ***N*-Benzoylglycyl-L-histidyl-L-leucine** (**Bz-GlyHisLeu** (**5**)), **and *N*-(Benzyloxycarbonyl)-L-phenylalanyl-L-histidyl-L-leucine** (**Z-PheHisLeu** (**6**)). The compound **2a** was obtained from Sigma Chemical Co., **3a** and **6** were obtained from Vega Chemicals, and **5** was obtained from Aldrich Chemical Co., and these compounds were used without further purification. The compounds **4a** and **4b** were prepared by reactions of corresponding *N*-hydroxysuccinimide esters of *N*-(benzyloxycarbonyl)amino acids with histidine.[3d]

***N*-Tetradecanoyl-L-histidine** (**MyrHis** (**2b**)) **and *N*-Tetradecanoyl-L-histidyl-L-leucine** (**MyrHisLeu** (**3b**)). The compounds **2b** and **3b** were prepared by the acylation of L-histidine (Wako Chemicals) and L-histidyl-L-leucine (Protein Research Foundation) with tetradecanoyl chloride in a way similar to the previous method.[12] Satisfactory elemental analyses were obtained. **2b**: mp 196 °C dec (lit.[12] mp 192 °C dec). Anal. Calcd for $C_{20}H_{35}N_3O_3$: C, 65.75; H, 9.59; N, 11.51. Found: C, 65.87; H, 9.61; N, 11.30. **3b**: mp 212–214 °C. Anal. Calcd for $C_{26}H_{46}N_4O_4$: C, 65.24; H, 9.69; N, 11.71. Found: C, 65.03; H, 9.63; N, 11.60.

Ditetradecyldimethylammonium Bromide ($2C_{14}Br$ (**7a**)), **Dihexadecyldimethylammonium Bromide** ($2C_{16}Br$ (**7b**)), **and Dihexadecyldimethylammonium Chloride** ($2C_{16}Cl$ (**7c**)). The surfactants **7a–7c** were prepared by reaction of the *N*,*N*-dimethylalkylamine and the corresponding alkyl bromide or chloride in refluxing ethanol in the presence of sodium carbonate and purified by recrystallizations from ethyl acetate as described previously.[13] Satisfactory elemental analyses were obtained for **7a–7c**. **7a**: Anal. Calcd for $C_{30}H_{64}NBr$: C, 69.44; H, 12.46; N, 2.98. Found: C, 69.18; H, 12.52; N, 2.68. **7b**: Anal. Calcd for $C_{34}H_{72}NBr$: C, 71.02; H, 12.65; N, 2.44. Found: C, 70.46; H, 12.49; N, 2.52. **7c**: Anal. Calcd for $C_{34}H_{72}NCl$: C, 76.99; H, 13.68; N, 2.64. Found: C, 76.83; H, 13.81; N, 2.52.

Commercially available hexadecyltrimethylammonium bromide (CTAB (**8a**)) and hexadecyltrimethylammonium chloride (CTA-Cl (**8b**)) were recrystallized from an ahydrous ethanol–ether mixture.

Kinetic Measurements. Rates of *p*-nitrophenol liberation from *p*-nitrophenyl esters were measured at 400 nm with a Hitachi 150-20 UV spectrophotometer. Each run was initiated by adding an acetonitrile solution (0.01 mL) of a substrate ester to a reaction medium of tris(hydroxymethyl)aminomethane (Tris) bufer (3.40 mL) containing both nucleophile and surfactant. The reaction obeyed the usual pseudo-first-order rate law, and the apparent second-order rate constant ($k_{a,obsd}$) for the hydrolysis of an ester substrate was evaluated by eq 1, where k_t

$$k_{a,obsd} = (k_t - k_s)/[\text{nucleophile}]_0 \quad (1)$$

and k_s refer, respectively, to the observed first-order rate constants for the hydrolytic cleavage (hydrolysis) of D(L)-S_n (n = 2, 12) and D(L)-ZS with and without a nucleophile and $[\text{nucleophile}]_0$ indicates the initial nucleophile concentration.

The clear stock solutions were prepared by dissolving both nucleophile and surfactant in Tris–KCl buffer with sonication (Bransonic 12, Yamato Scientific Co.) at 50 °C for 1 h.

Fluorescence Measurements. Polarization. The fluorescence spectra were measured on a Union Giken FS-501A fluorescence polarization spectrophotometer with a Sord microcomputer M200 Mark II; the emission at 430 nm originating from 1,6-diphenyl-1,3,5-hexatriene (DPH) was monitored upon excitation at 360 nm with a slit width of 3.5 nm

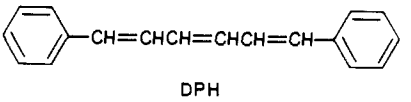

DPH

(10) Bodansky, M.; Vigneaud, V. d. *J. Am. Chem. Soc.* **1959**, *81*, 6072.
(11) Ingles, D. W.; Knowles, J. R. *Biochem. J.* **1967**, *104*, 369.
(12) Gitler, C.; Ocoa-Solano, A. *J. Am. Chem. Soc.* **1968**, *90*, 5004.
(13) Okahata, Y.; Ando, R.; Kunitake, T. *Bull. Chem. Soc. Jpn.* **1979**, *52*, 3647.

for both excitation and emission sides. The fluorescence polarization (P) of DPH was measured after sonication of the surfactant solution, and calculated by eq 2, where I is the fluorescence intensity and the subscripts

$$P = (I_{vv} - C_f I_{vv})/(I_{vv} + C_f I_{vh}) \quad (2)$$

v and h refer to the orientations, vertical and horizontal, respectively, for the excitation and analyzer polarizers in this sequence: e.g., I_{vh} indicates the fluorescence intensity measured with a vertical excitation polarizer and a horizontal analyzer polarizer.[14,15] C_f is the grating correction factor, given by I_{hv}/I_{hh}.

Micropolarity. Steady-state fluorescence spectra were obtained on a SLM 4800 spectrometer (Xe lamp) at 25 °C; the emission spectra were monitored upon excitation at 337 nm with a slit width of 0.5 and 8 nm for excitation and emission sides, respectively. The fluorescence intensity was measured by the use of pyrene (Py: 5×10^{-5} M) as a probe after sonication of the surfactant solution. The intensity ratio of Py fluorescence peaks (I_{385}/I_{375}) reflects the polarity of the pyrene's microenvironment.[16]

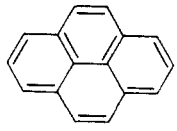

pyrene

Light-Scattering Measurements. In recent years, the modified version of classical light scattering, quasi-elastic or dynamic light scattering, has been used to determine the size and shape of surfactant aggregates in aqueous solution,[17,18] so we have employed the light-scattering measurements in order to evaluate the hydrodynamic diameters (d_{hy}) of micelles, vesicles, and coaggregates.

The dynamic light-scattering measurements were performed with a Nicomp Model TC-100 computing autocorrelator, an argon laser light source (488 nm), a variable angle adjustment apparatus, and a Hazeltin microcomputer that used the cumulant program and directly afforded d_{hy} of the aggregates as described previously.[19] All surfactant solutions were prepared in aqueous solutions identical with those used in the kinetic studies and were filtered through a 0.45 μm Bio-Rad polycarbonate filter before being measured. The solutions containing the vesicular surfactant were used for the measurements after sonication at 50 °C for 30 min with a Braun-Sonic Model 1510 apparatus (80 W).

Electronic Microscopy. Electron micrographs were obtained by means of negative-staining and freeze-fracture techniques. In the negative-staining method, a sample solution (200 μL) of lipid aggregates in Tris buffer containing KCl was mixed with a 2% (w/w) aqueous solution of uranyl acetate (200 μL), sonicated for 60 min with a bath-type sonicator (Bransonic 12) at 80 W and 50 °C. The sample was then applied to a carbon grid and dried overnight in a vacuum desiccator at room temperature. Preparations of freeze-fracture replicas were similar to those described elswhere.[15] Electron micrographs were taken on a JEOL JEM-2000FX electron microscope, installed at the Research Laboratory for High Voltage Electron Microscopy of Kyushu University.

Circular Dichroism. The CD spectra of peptide catalysts were recorded with a Jasco J-50A recording spectropolarimeter (Xe lamp, 1.0-cm cell) at room temperature.

Results and Discussion

Temperature Effects in the Vesicular Systems. The temperature dependence of enantioselectivity (reflected in $k^L_{a,obsd}/k^D_{a,obsd}$) for the hydrolysis of D(L)-ZS, D(L)-S_2, and D(L)-S_{12} catalyzed by MyrHisLeu in the presence of $2C_{14}Br$ is shown in Figure 1A. It is noteworthy that the temperature dependence of enantioselectivity for the hydrolysis of S_{12}, which bears a long acyl chain, was bell-shaped with a maximum ($k^L_{a,obsd}/k^D_{a,obsd} = 11$) at 25 °C. The

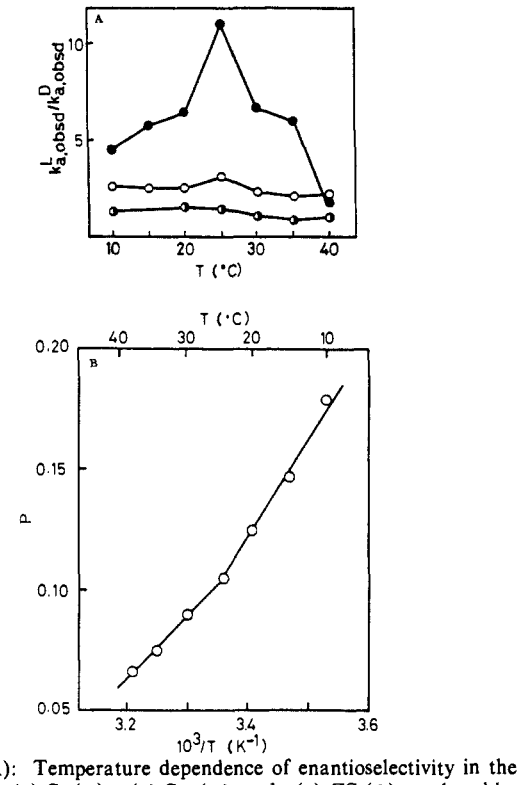

Figure 1. (A): Temperature dependence of enantioselectivity in the hydrolysis of D(L)-S_2 (◑), D(L)-S_{12} (●), and D(L)-ZS (○) catalyzed by MyrHisLeu + $2C_{14}Br$ at pH 7.6 (0.08 M Tris-KCl buffer) in 3% (v/v) CH_3CN-H_2O. [MyrHisLeu] = 3×10^{-5} M, [substrate] = 1×10^{-5} M, [$2C_{14}Br$] = 1×10^{-3} M. (B): Correlation between fluorescence polarization (P) of DPH and temperature in vesicles of $2C_{14}Br$ at pH 7.6 (0.08 M Tris-KCl buffer). [DPH] = 1×10^{-7} M, [$2C_{14}Br$] = 1×10^{-3} M.

phase-transition (gel to liquid-crystalline) temperature (maximum temperature, T_m) was observed at 14.5 °C (lit.[20] T_m 16 °C) for the Tris-KCl buffer solution of $2C_{14}Br$ by differential scanning calorimetry (DSC).[21] Interestingly, the optimum temperature (25 °C) for the maximum enantioselectivity was somewhat higher than the T_m value[20] for the aqueous solution of $2C_{14}Br$ evaluated by the DSC method. On the other hand, the enantioselectivity in the hydrolysis of S_2, which has a short chain, is almost constant over the whole temperature range examined. The hydrolysis of ZS, which has a bulky side group, tends to be bell-shaped with a gentle maximum at 25 °C in the bilayer catalytic system of $2C_{14}Br$. The magnitude of the enantioselectivity for the long-chained substrate (S_{12}) is considerably larger than for the short-chained substrates (S_2, ZS). These results suggest that hydrophobic interactions between the substrate and the nucleophile are of great importance for the enhancement of enantioselectivity. Interestingly, the enantioselectivity for the hydrolysis of all the substrates (S_2, S_{12}, ZS) employed converged to a low value at 40 °C in the bilayer systems of $2C_{14}Br$. Probably, this can be attributed to the fact that the highly oriented membrane structure becomes increasingly disordered at higher temperatures.

It is known that the results obtained by fluorescence measurements agree well with data from NMR and DSC measurements in terms of the mobility of molecules in microenvironments and the phase transition from gel to liquid-crystalline states.[22] Thus, the fluorescence polarization of DPH in $2C_{14}Br$ surfactants is shown in Figure 1B. Although DPH does not dissolve in water, a great increase in fluorescence intensity was observed after it was mixed with the surfactant, indicating solubilization of DPH into

(14) Azumi, T.; McGlynn, S. P. *J. Chem. Phys.* **1962**, *37*, 2413.
(15) Murakami, Y.; Kikuchi, J.; Takaki, T.; Uchimura, K.; Nakano, A. *J. Am. Chem. Soc.* **1985**, *107*, 2161.
(16) Kalyanasundaram, K.; Thomas, J. K. *J. Am. Chem. Soc.* **1977**, *99*, 2039.
(17) Mazer, N. A.; Carey, M. C.; Benedek, G. B. *Micellization, Solubilization and Microemulsions*; Mittal, K. L., Ed.; Plenum: New York, 1977; Vol. 1, p 359.
(18) Nicoli, D. F.; Dorshow, R. B.; Bunton, C. A. *Surfactants in Solution* Mittal, K. L., Lindman, B., Eds.; Plenum: New York, 1984; Vol. 1, p 455 and references cited therein.
(19) Moss, R. A.; Chiang, Y.-C.; Hui, Y. *J. Am. Chem. Soc.* **1984**, *106*, 7506.
(20) The T_m values were determined to be 16 and 28 °C for aqueous solutions of $2C_{14}Br$ and $2C_{16}Br$, respectively, by DSC as described in: Okahata, Y.; Ando, R.; Kunitake, T. *Ber. Bunsenges. Phys. Chem.* **1981**, *85*, 789.
(21) DSC was conducted with a Daini-Seikosha SSC-560U instrument by courtesy of Prof. T. Kunitake of Kyushu University. The temperature was raised from 0 °C at a rate of 2 °C/min.
(22) Nagamura, T.; Mihara, S.; Okahata, Y.; Kunitake, T.; Matsuo, T. *Ber. Bunsenges. Phys. Chem.* **1978**, *82*, 1093.

Table I. Rate Constants ($k_{a,obsd}$, M^{-1} s^{-1}) and Enantioselectivity ($k^L_{a,obsd}/k^D_{a,obsd}$) for the Hydrolysis of S_n by L-Histidine Derivatives in the Vesicular ($2C_{14}Br$) Systems[a]

catalyst	L-ZS	D-ZS	L/D[b]	L-S_{12}	D-S_{12}	L/D[b]
Z-His (**2a**)	10	9	1.1	46	31	1.5
MyrHis (**2b**)	930	370	2.5	1800	340	5.3
Z-HisLeu (**3a**)	14	10	1.4	47	47	1.0
Z-HisPhe (**3c**)	56	28	2.0	92	41	2.2
MyrHisLeu[c] (**3b**)	190	60	3.2	560	50	11
Z-LeuHis (**4a**)	210	46	4.6	1400	63	22
Z-PheHis (**4b**)	480	110	4.4	4300	170	25
Bz-GlyHisLeu (**5**)	2	2	1.0	45	34	1.3
Z-PheHisLeu (**6**)	260	62	4.2	1700	63	27

[a] Conditions: 25 °C; pH 7.6; 0.08 M Tris buffer (0.08 M KCl); 3% (v/v) CH_3CN–H_2O; [cat.] = 5×10^{-5} M, [S_n] = 1×10^{-5} M, [$2C_{14}Br$] = 1×10^{-3} M. [b] These values are enantioselective parameters, which include the experimental error within ±5%. [c] [MyrHisLeu] = 3×10^{-5} M.

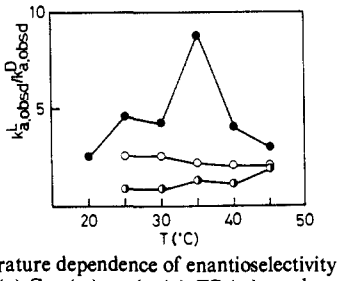

Figure 2. Temperature dependence of enantioselectivity in the hydrolysis of D(L)-S_2 (◑), D(L)-S_{12}, (●), and D(L)-ZS (○) catalyzed by MyrHisLeu + $2C_{16}Br$ at pH 7.6 (0.08 M Tris–KCl buffer) in 3% (v/v) CH_3CN–H_2O. [MyrHisLeu] = 3×10^{-5} M, [substrate] = 1×10^{-5} M, [$2C_{14}Br$] = 1×10^{-3} M.

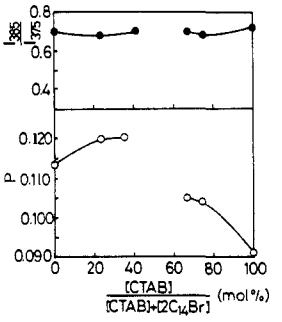

Figure 3. Correlation between fluorescence polarization (P) of DPH (○) or micropolarity (I_{385}/I_{375}, ●) and coaggregate composition at 25 °C and pH 7.6 (0.08 M Tris–KCl buffer). [$2C_{14}Br$] = 1×10^{-3} M.

the hydrophobic region of the aggregates. The fluorescence depolarization is caused by molecular motion of the probe, which reflects the microviscosity of the surrounding region. Therefore, the temperature dependence of the polarization indicates that the fluidity of the hydrophobic region changes with temperature, as shown in Figure 1B. The degree of polarization in the $2C_{14}Br$ sample does not show clear, abrupt changes but appears to decrease more sharply in the temperature range of 10–20 °C and decrease more gently in the temperature range of 30–40 °C. A minor change in polarization was observed around 25 °C.

Interestingly, the highest enantioselectivity was also observed at 25 °C for the hydrolysis of the hydrophobic substrate (S_{12}) in the vesicular system of MyrHisLeu + $2C_{14}Br$ as was shown in Figure 1A. The inflection observed at about 25 °C in the correlation of P against temperature suggests that the fluidity of the membrane matrix of $2C_{14}Br$, which is closely related to the hydrophobic microenvironment, is delicately changed around 25 °C, somewhat higher than the maximum temperature (14.5 °C) for the phase transition of $2C_{14}Br$.

A similar trend was observed in the bilayer system of MyrHisLeu + $2C_{16}Br$ as shown in Figure 2. The optimum temperature (35 °C) for the maximum enantioselectivity in the hydrolysis of the long-chain enantiomers (D(L)-S_{12}) was somewhat higher than the T_m value of $2C_{16}Br$ (28 °C),[20] and the enantioselectivity converged to a reduced magnitude at 45 °C. From these common temperature effects, we supposed that the optimum temperatures (25 °C for $2C_{14}Br$ and 35 °C for $2C_{16}Br$) might present appropriate hydrophobic microenvironments (which are not as hard as the gel state and not as soft as the liquid-crystalline one) and result in the amplification of efficient recognition between catalyst (MyrHisLeu) and substrate (L-S_{12}).

Effect of Amino Acid Sequence in Peptide Catalysts. It is well-known that the amino acid sequence in enzymes is biologically crucial for development of catalytic activity and molecular recognition. In this study, we examined the catalytic efficiency and enantioselectivity for the hydrolysis of D(L)-ZS and D(L)-S_{12} by using various L-histidine derivatives, including *N*-acyl-L-histidine, dipeptide, and tripeptide in the vesicular systems ($2C_{14}Br$). The results are summarized in Table I. The noteworthy aspects are as follows: With respect to the hydrophobicity of the reactants, (a) the hydrophobic acyl chain (*N*-tetradecanoyl) in catalysts (MyrHis, MyrHisLeu) plays an important role for the enhancement of rate and stereoselectivity (MyrHis ≫ Z-His and MyrHisLeu ≫ Z-HisLeu). In particular, the long-chain dipeptide catalyst MyrHisLeu presented a remarkably high enantioselectivity ($k^L_{a,obsd}/k^D_{a,obsd}$ = 11) for the hydrolysis of the long-chain substrates S_{12}. On the other hand, with respect to location of the histidine (His) unit, (b) the dipeptide catalysts (Z-*His*Leu, Z-*His*Phe) with the His unit directly attached to the Z group, were not much more efficient for the enhancement of catalytic efficiency (reflected in $k_{a,obsd}$) and stereoselectivity than Z-His alone; (c) the dipeptides Z-Leu*His* and Z-Phe*His* where the His unit is attached to the C terminal dramatically enhance the rate and enantioselectivity ($k^L_{a,obsd}/k^D_{a,obsd}$ = 22 and 25) for the hydrolysis of the long-chain enantiomeric substrates S_{12}; (d) the tripeptide Z-Phe*His*Leu where the His is in the middle position was most efficient for the enhancement of enantioselectivity (affording $k^L_{a,obsd}/k^D_{a,obsd}$ = 27) among all the catalysts employed in this study, but Bz-Gly*His*Leu was not efficient. With respect to the position of a phenylalanine (Phe) unit, (e) the Phe unit in Z-*Phe*His and Z-*Phe*HisLeu, attached directly to the Z group, played an important role in enhancing the rate and enantioselectivity for the hydrolysis of S_{12}. The foregoing results suggest that the hydrophobicity and location of L-His and L-Phe units in the catalyst, and the hydrophobicity of the L-S_{12} substrate (bearing a L-Phe unit) are of great importance for rate and enantioselectivity, through the hydrophobic and/or recognizant interactions between the catalyst and substrate, both carrying common L-Phe units.

Composition Effect of Vesicles and Micelles. It is of interest that the tripeptide Z-PheHisLeu is the most effective catalyst for the enhancement of enantioselectivity among the catalysts shown in Table I. We examined the effect of the composition of the aggregates on the enantioselective hydrolysis of D(L)-ZS and D(L)-S_{12} catalyzed by Z-PheHisLeu. The kinetic results are summarized in Table II. The noteworthy aspects are as follows: (a) The rate for the hydrolysis of D(L)-S_{12} was almost bell-shaped with a maximum at a CTAB concentration of 23 mol % (the concentration of CTAB is expressed as mole percent of total surfactant), though such a behavior was not observed for the hydrolysis of D(L)-ZS. Surprisingly, this behavior resembles the bell-shaped fluorescence polarization of 1,6-diphenyl-1,3,5-hexatriene (DPH) as a fluorescent probe[14,15] (Figure 3) under the

Table II. Rate Constants ($k_{a,obsd}$, M^{-1} s^{-1}) and Enantioselectivity ($k^L_{a,obsd}/k^D_{a,obsd}$) for the Hydrolysis of S_n by Z-PheHisLeu in the Coaggregate Systems Composed of $2C_{14}Br$ and CTAB Surfactants[a]

[CTAB]/([CTAB] + [$2C_{14}Br$]), mol %		L-ZS	D-ZS	L/D	L-S_{12}	D-S_{12}	L/D
		260	62	4.2	1700	63	27
0	(cat., Z-PheHis)	480	110	4.4	4300	170	25
	(cat., Z-LeuHis)	210	46	4.6	1400	63	22
9		260	62	4.2	1700	59	29
23		240	54	4.4	2000	78	26
33		200	46	4.3	1400	42	33
41		200	35	5.7	1100	21	52
		86	8.0	*11*	780	11	*71*
67	(cat., Z-PheHis)	150	35	4.2	2500	120	21
	(cat., Z-LeuHis)	160	42	3.9	870	42	21
71		45	7.8	5.8	380	8.0	48
75		36	8.5	4.2	340	8.0	43
83		30	7.5	4.0	360	21	17
100[b]		30	10	3.0	290	16	18

[a] The rate constants have maximum errors of ±4%. Conditions: 25 °C; pH 7.6; 0.08 M Tris buffer (0.08 M KCl); 3% (v/v) CH_3CN–H_2O; [Cat.] = 5×10^{-5} M, [$2C_{14}Br$] = 1×10^{-3} M, [S_n] = 1×10^{-5} M. [b] [CTAB] = 3×10^{-3} M.

same conditions as described in Table II. This suggests that the fluidity of the hydrophobic region of $2C_{14}Br$ vesicles changes upon addition of CTAB[22] and results in a large rate enhancement for the long-chain substrates (D(L)-S_{12}) at the CTAB concentration of 23 mol %. On the other hand, the micropolarity in the hydrophobic regions of the aggregates, as reflected in the ratio of the intensity of pyrene at 385 nm (I_{385}) relative to that at 375 nm (I_{375}),[16] appeared to be almost constant (I_{385}/I_{375} = 0.68–0.72) over the whole composition range of the coaggregates, as shown in Figure 3. (b) The enantioselectivity ($k^L_{a,obsd}/k^D_{a,obsd}$ = 27 and 4.2 for the hydrolysis of S_{12} and ZS, respectively) in the pure vesicular system of $2C_{14}Br$ is dramatically enhanced by adding CTAB and reaches an enantiomer rate constant ratio = 71 (for S_{12}) and 11 (for ZS) at the CTAB concentration of 67 mol %. This large enhancement of enantioselectivity can be mainly attributed to a more reduced rate of hydrolysis of the D isomers compared with the L isomers. In the relation to (b), no effect of added CTAB (67 mol % CTAB) was observed for the dipeptide catalysts (Z-PheHis, Z-LeuHis) in $2C_{14}Br$–CTAB as described in Table II. This implies that the structure or conformation of the tripeptide catalyst (Z-PheHisLeu) is also crucial along with the composition of the coaggregates. The coaggregates composed of 67 mol % CTAB and 33 mol % $2C_{14}Br$ present an appropriate microenvironment for the enhancement of enantioselective hydrolysis. (c) No clear solution was obtained in the CTAB concentration range from 41 to 67 mol % (separation occurs in this region), but very high enantioselectivity ($k^L_{a,obsd}/k^D_{a,obsd}$ = 52 and 71) is obtained on the verge of phase separation.

The composition effect of coaggregates on the enantioselective hydrolysis of D(L)-S_{12} with Z-PheHisLeu was also investigated with a cationic coaggregate system composed of $2C_{16}Cl$ and CTA–Cl surfactants, as described in Table III. The reaction conditions are the same as those shown in Table I. Both $k_{a,obsd}$ and $k^L_{a,obsd}/k^D_{a,obsd}$ values increased in the CTA–Cl concentration range of 0–23 mol % and decreased in the range of 23–100 mol % CTA–Cl. As a result, not only the rate but also enantioselectivity was maximized at the 23 mol % CTA–Cl concentration. It is noteworthy that remarkable stereochemical control of the enantioselective hydrolysis was obtained simply by adjusting the composition of the coaggregates formed from cationic double-chain ($2C_{14}Br$, $2C_{16}Cl$) and cationic single-chain (CTAB or CTA–Cl) surfactants.

As it seemed that the enantioselectivity responds directly and sensitively to variations in coaggregate structure that can be monitored by dynamic light scattering (dls), we investigated the apparent hydrodynamic diameter (d_{hy}) of coaggregates in order to consider the relation of d_{hy} to the enantioselectivity.[1c] In Figure 4, we plot the enantioselectivity on the left-hand ordinate and d_{hy} on the right-hand ordinate, both versus the $2C_{14}Br$–CTAB coaggregate composition on the abscissa. The d_{hy} data were collected at a 90° scattering angle and were reproducible to better than ±10% in duplicate preparations. The remarkable similarity in the dependence of both d_{hy} and enantioselectivity on coaggregate composition is immediately obvious. Moreover, it is suggested that the increasing correlated, extended molecular alignment within coaggregates on the verge of phase separation may impose ordered relative arrangements on solubilized catalyst and substrate molecules, thus engendering amplified enantioselectivity.

Interestingly, a similar relationship between d_{hy} and enantioselectivity is obtained in the coaggregate system of $2C_{16}Cl$

Table III. Rate Constants ($k_{a,obsd}$, M^{-1} s^{-1}) and Enantioselectivity ($k^L_{a,obsd}/k^D_{a,obsd}$) for the Hydrolysis of D(L)-S_{12} by Z-PheHisLeu in the Coaggregate System Composed of $2C_{16}Cl$ and CTA-Cl Surfactants[a]

[CTA-Cl]/([CTA-Cl] + [$2C_{16}Cl$]), mol %	L-S_{12}	D-S_{12}	L/D
0	1000	40	25
10	1200	43	28
23	2000	60	*33*
36	1500	64	23
50	870	48	18
67	580	41	14
100[b]	200	26	7.7

[a] The rate constants have maximum errors of ±3%. Conditions: 25 °C; pH 7.6; 0.02 M Tris buffer (0.02 M KCl); 3% (v/v) CH_3CN–H_2O; [D(L)-S_{12}] = 1×10^{-5} M, [Z-PheHisLeu] = 1×10^{-4} M, [$2C_{16}Cl$] = 1×10^{-3} M. [b] [CTA-Cl] = 2×10^{-3} M.

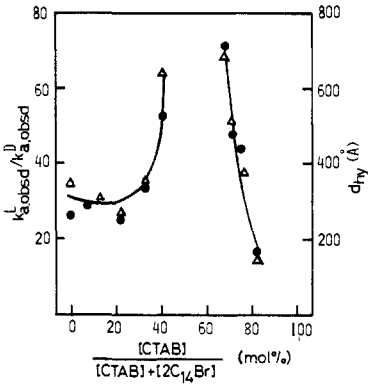

Figure 4. Enantioselectivity ($k^L_{a,obsd}/k^D_{a,obsd}$) for the hydrolysis of D-(L)-S_{12} by Z-PheHisLeu (●, left-hand ordinate) and apparent hydrodynamic diameter (d_{hy}) of the coaggregates (△, right-hand ordinate) versus coaggregate composition (mole percent CTAB in mixture of $2C_{14}Br$ and CTAB, abscissa) at 25 °C and pH 7.6 (0.08 M Tris–KCl buffer) in 3% (v/v) CH_3CN–H_2O. [Z-PheHisLeu] = 5×10^{-5} M, [D(L)-S_{12}] = 1×10^{-5} M, [$2C_{14}Br$] = 1×10^{-3} M.

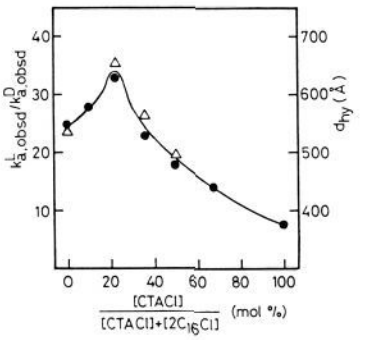

Figure 5. Enantioselectivity ($k^L_{a,obsd}/k^D_{a,obsd}$) for the hydrolysis of D-(L)-S_{12} by Z-PheHisLeu (●, left-hand ordinate) and apparent hydrodynamic diameter (d_{hy}) of the coaggregates (△, right-hand ordinate) versus coaggregate composition (mole percent CTA–Cl in mixture of $2C_{16}Cl$ and CTA–Cl, abscissa) at 25 °C and pH 7.6 (0.02 M Tris–KCl buffer) in 3% (v/v) CH_3CN–H_2O. [Z-PheHisLeu] = 1×10^{-4} M, [D(L)-S_{12}] = 1×10^{-5} M, [$2C_{16}Cl$] = 1×10^{-3} M.

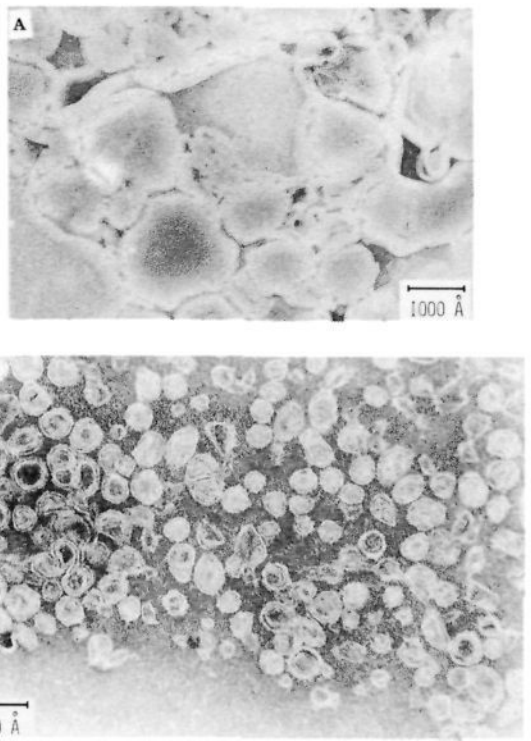

Figure 6. Electron micrographs, negatively stained with uranyl acetate, for (A) $2C_{14}Br$ and (B) coaggregates of 41 mol % CTAB and 59 mol % $2C_{14}Br$.

vesicles and CTA–Cl micelles as shown in Figure 5. In this case, however, the maximal enantioselectivity does not appear adjacent to a patent phase boundary of the coaggregate system of $2C_{16}Cl$ + CTA–Cl as it did with $2C_{14}Br$ + CTAB (Figure 4). However, dls indicates very large (8500–10 000 Å), unstable "growing" aggregates in the 50–100 mol % CTA–Cl region, so that the maxima in d_{hy} and enantioselectivity do lie reasonably close to coaggregate composition in which correlated and extended molecular ordering is obtained. It is worth noting that the size and curvature of the coaggregates should play an important role in the enhancement of enantioselectivity and might be related to the hydrophobicity and fluidity of the coaggregate matrix.

Furthermore, most remarkably, the diastereoselectivity of *p*-nitrophenyl *N*-(carbobenzyloxy)-L(D)-prolyl-L-prolinate cleavage by *N*-(*n*-cetyl)-*N*,*N*-dimethyl[*β*-(3-carboxy-4-iodosobenzoxy)-ethyl]ammonium chloride in $2C_{16}Cl$–CTA–Cl coaggregates shows an identical dependence of d_{hy} and peaks at the same coaggregate composition.[1d] Further experimental details will be described elsewhere.

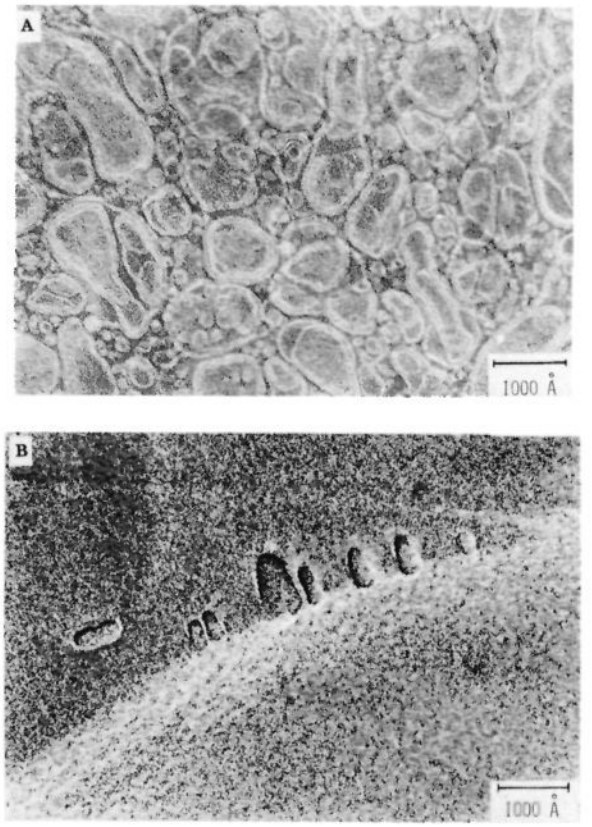

Figure 7. Electron micrographs for coaggregates of 67 mol % CTAB and 33 mol % $2C_{14}Br$: A, negative staining method; B, freeze–fracture technique.

Table IV. Angular Dependence of Apparent Hydrodynamic Diameter (Å) of Vesicles and Coaggregates[a]

[CTAB]/([CTAB] + [$2C_{14}Br$]), mol %	angle, deg				
	45	60	90	120	135
0	400	380	380	390	380
13	300	330	310	300	300
33	320	320	330	310	310
41	700	650	630	630	630
67	1600	1400	680	600	630
75	330	370	380	360	350
83	200	160	130	110	120

[a] The value of the diameter has a maximum error of ±10%. Conditions: pH 7.6; 0.08 M Tris buffer (0.08 M KCl); [$2C_{14}Br$] = 1×10^{-3} M.

Morphology of the Coaggregates. An attractive finding of this study is that the magnitude of the enantioselectivity agrees fairly well with the hydrodynamic diameter of the coaggregates at a 90° scattering angle, although the morphology of coaggregates could not be determined in this way. Therefore, we examined the morphology of the coaggregates composed of $2C_{14}Br$ and CTAB on the basis of both electron microscopy and dls data.

First, we observed the aggregate morphology by electron microscopy as shown in Figures 6 and 7. The electron micrograph of negatively stained aggregates of $2C_{14}Br$ (Figure 6A) shows the formation of lamella, which reflects the morphology after being allowed to stand for 1 day at room temperature. With respect to the coaggregates composed of 59 mol % $2C_{14}Br$ and 41 mol % CTAB, the electron micrograph (Figure 6B) shows the presence of single- and double-walled vesicles in the diameter range of 200–600 Å. The electron micrographs of 33 mol % $2C_{14}Br$/67 mol % CTAB coaggregates are given in Figures 7A (negatively stained method) and 7B (freeze–fracture technique).[23] As shown in Figure 7A, large and elongated coaggregates including small

(23) The freeze-fracture replicas were prepared by courtesy of Prof. T. Kunitake.

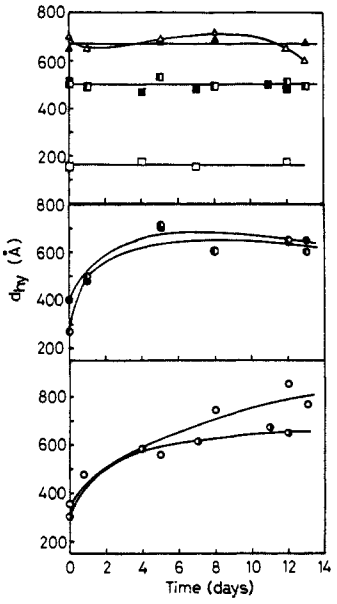

Figure 8. Time courses of d_{hy} change for $2C_{14}Br$ vesicles (○), coaggregates containing 13 (◑), 23 (◐), 33 (●), 41 (▲), 67 (△), 71 (■), 75 (◧), and 83 mol % (□) CTAB micelles.

particles were observed. On the other hand, the micrograph of the freeze–fracture replica clearly showed the presence of elliptical aggregates with various long diameters of 200–1000 Å (Figure 7B).

Second, we examined variable angle (45–135°) dls within 4 h after sonication of samples in order to study the shape of the aggregates. The results are summarized in Table IV. No angular dependence of d_{hy} was observed for the pure vesicles of $2C_{14}Br$ or coaggregates containing 13, 33, and 75 mol % CTAB; so that the shapes of these aggregates are estimated to be nearly spherical vesicles or micelles with diameters of 300–400 Å. Interestingly, we found that the 59 mol % $2C_{14}Br$/41 mol % CTAB coaggregates are large and spherical particles with hydrodynamic diameters (ca. 650 Å) in good agreement with the observed maximum particle diameter by electron microscopy as shown in Figure 6B. On the other hand, coaggregates containing 67 and 83 mol % CTAB micelles are characterized by a strong dependence of d_{hy} on the scattering angle and are presumably rodlike[24] or elongated coaggregates, although the size of the former (600–1600 Å) is 5–8 times as large as the latter (110–200 Å). Note that the 67 mol % CTAB coaggregates are most efficient for enantioselective hydrolysis reactions as described above.

Finally, the stability of the coaggregates was examined by following the time course of d_{hy} change with dls at a fixed angle of 90° as shown in Figure 8. There are a few reports about the time course of change in morphology of dialkylammonium bilayers.[25] In relation to the dialkylammonium $2C_{14}Br$ vesicles, it is noteworthy that the d_{hy} value gradually increased with time; the size doubled after 2 weeks. On the other hand, no time-dependent d_{hy} changes were observed for the coaggregates containing 41 and 71–83 mol % CTAB, and these coaggregates are very stable for at least 2 weeks. Interestingly, the coaggregates composed of 33 mol % $2C_{14}Br$ and 67 mol % CTAB were unstable, and this might be related to the variable shapes of this composition shown by the electron micrographs in Figure 7A.

Origin of Enantioselectivity. There have been only a few reports of the relation between stereoselectivity and the conformation of peptide catalysts for the enantioselective hydrolysis of amino acid esters,[26] though the helical structure of polypeptides and cyclo-

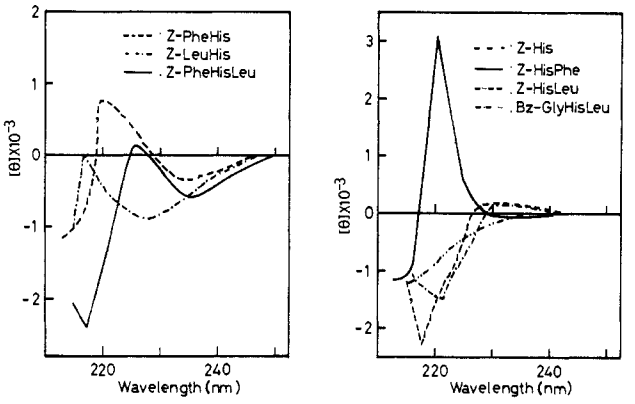

Figure 9. CD spectra of peptide catalysts with $2C_{14}Br$ vesicles in 5% (v/v) CH_3OH–H_2O. [cat.] = 2.5 × 10^{-4} M, [$2C_{14}Br$] = 1 × 10^{-3} M.

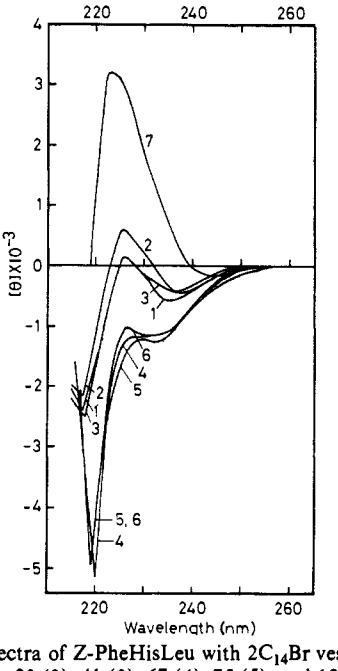

Figure 10. CD spectra of Z-PheHisLeu with $2C_{14}Br$ vesicles (1), coaggregates containing 23 (2), 41 (3), 67 (4), 75 (5), and 100 mol % CTAB micelles (6), and in methanol (7). [Z-PheHisLeu] = 2.5 × 10^{-4} M, [$2C_{14}Br$] = 1 × 10^{-3} M.

peptides has been discussed in detail on the basis of CD experiments.[27]

The CD spectra of peptide catalysts employed in this study were measured in the presence of $2C_{14}Br$ vesicles, as shown in Figure 9. Interestingly, the specific CD spectra at ca. 235 nm occured in the active peptides (Z-PheHisLeu, Z-PheHis) with $2C_{14}Br$ vesicles, which promoted the enantioselectivity for the hydrolysis of the long-chain enantiomers (D(L)-S_{12}). On the other hand, no specific CD spectrum at 235 nm was obtained in any of the inactive peptides (Z-His, Z-HisPhe, Z-HisLeu, Bz-GlyHisLeu) or in the active Z-LeuHis peptide. It is also noteworthy that the CD patterns of the active peptides (Z-PheHisLeu, Z-PheHis, Z-LeuHis) and the inactive Bz-GlyHisLeu in the presence of $2C_{14}Br$ and in methanol differ remarkably from each other, though there is not much difference between the CD patterns with $2C_{14}Br$ and those in methanol in the cases of inactive peptides (Z-His, Z-HisPhe, Z-HisLeu) (data are not shown). These imply that these specific CD spectra at ca. 235 nm in Z-PheHisLeu and Z-PheHis bound to vesicles of $2C_{14}Br$ may support the left-handed rigid conformation of the common unit of L-Phe-L-His through the intramolecular interaction between L-Phe and L-His residues.[28]

(24) Ikeda, S.; Hayashi, S.; Imae, T. *J. Phys. Chem.* **1981**, *85*, 106.
(25) Kunitake, T. *J. Macromol. Sci. Chem.* **1979**, *A13*(5), 587.
(26) (a) Kikuchi, K.; Tanihara, M.; Imanishi, Y. *Int. J. Biol. Macrmol.* **1982**, *4*, 305. (b) Tanihara, M.; Imanishi, Y. *Polym. J. (Toyko)* **1983**, *15*, 509. (c) Ueoka, R.; Matsumoto, Y.; Nagamine, K.; Yasui, H.; Harada, K.; Sugii, A. *Chem. Pharm. Bull.* **1987**, *35*, 3070.

(27) (a) Sisido, M.; Egusa, S.; Imanishi, Y. *J. Am. Chem. Soc.* **1985**, *105*, 4077. (b) Egusa, S.; Takaki, J.; Sisido, M.; Imanishi, Y. *Bull. Chem. Soc. Jpn.* **1986**, *59*, 2195.

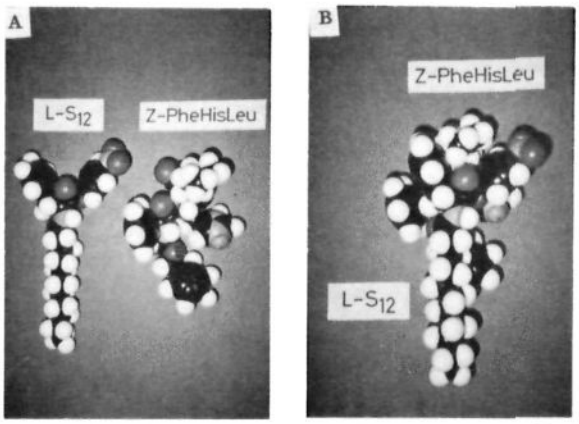

Figure 11. Space-filling molecular model of Z-PheHisLeu or L-S_{12} (A) and a recognizant fitting model of Z-PheHisLeu and L-S_{12} (B).

The Phe, His, and Leu units in Z-PheHisLeu are well-known for forming a stable α-helical structure. And it has been already reported[26c] that the CD curve of this tripeptie with CTA–Cl micelles between 200 and 240 nm closely resembled those of α-helical peptides.[29] Therefore, we examined the schematic CD experiments for the active tripeptide (Z-PheHisLeu) by changing the composition of vesicular ($2C_{14}Br$) and micellar (CTAB) surfactants. As shown in Figure 10, the CD spectra of Z-PheHisLeu in the presence of surfactants were extremely different from that in methanol. Moreover, interestingly, it was found that the spectra for the pure vesicles of $2C_{14}Br$ and coaggregates containing 23 or 41 mol % CTAB were fairly different from those for the pure micelles of CTAB and coaggregates containing 25 or 33 mol % $2C_{14}Br$. These results suggest that the rigid conformation of Z-PheHisLeu (like an α-helical arrangement) in the pure CTAB miceller system[26c,29] could be held in the coaggregates composed of 33 mol % $2C_{14}Br$ and 67 mol % CTAB, which produced the highest enantioselectivity ($k^{L}_{a,obsd}/k^{D}_{a,obsd}$ = 71), though the rigid conformation might change to some extent in the pure (100% $2C_{14}Br$) and large (59 mol % $2C_{14}Br$/41 mol % CTAB) vesicles. It may be concluded that the change in the hydrophobic microenvironment should induce some conformational change of Z-PheHisLeu[26b] and the 33 mol % $2C_{14}Br$/67 mol % CTAB coaggregates presented an appropriate microenvironment for the marked enhancement of enantioselectivity as described in the section on composition effect of vesicles and micelles.

Here, we want to propose a rationale conformation of Z-PheHisLeu in the micellar and vesicular systems on the basis of CD experiments in this study. Figure 11 shows space-filling molecular models (CPK model) of Z-PheHisLeu and L-S_{12}. The side chains of L-Phe, L-His, and L-Leu in Z-PheHisLeu constitute a hydrophobic pocket through the intramolecular interactions between amino acid residues as well as hydrogen bonds between amide parts in the tripeptide catalyst. This idea of a hydrophobic pocket has been proposed for the enzyme catalysis[30] and used to explain the rapid hydrolysis of the specific substrate by synthesized cyclopeptides.[26b,31] An enzyme-like fitting of the specific substrate (L-S_{12}) and the active tripeptide (Z-PheHisLeu) through the efficient hydrophobic and/or recognizant interactions between the substrate and catalyst, both carrying common L-Phe units, is presented in Figure 11B. On the other hand, it is suggested from the CPK model that the interaction between D-Phe in substrate and L-Phe in catalyst might bring an unfavorable fitting in the course of reaction.

We wish to emphasize with respect to the origin of enantioselectivity that a favorable fitting of the L isomer substrate and the active tripeptide like "key and lock" should be very important to enhance the enantioselectivity, and subsequently, the adjusting of the hydrophobic microenvironment to the optimum fit of reactants by changing appropriately the composition of coaggregates would induce the highest enantioselectivity.

Conclusion. A summary of the noteworthy aspects of this study is as follows: (a) The enantioselectivity was greatly elevated at temperatures somewhat higher than the phase transition for the hydrolysis of long-chain enantiomers (D(L)-S_{12}) by the long-chain MyrHisLeu catalyst in the artificial membrane ($2C_{14}Br$, $2C_{16}Br$) systems. (b) The LLL-tripeptide (Z-PheHisLeu) was most efficient for the enhancement of enantioselectivity among all the peptide catalysts considered. (c) With respect to the reaction of D(L)-S_{12} with Z-PheHisLeu, excellent correlations were obtained between the stereoselectivity and the apparent mean hydrodynamic diameters of cationic coaggregates composed of double-chain ($2C_{14}Br$, $2C_{16}Cl$) and single-chain (CTAB, CTA–Cl) surfactants. Particularly, it is of interest that the coaggregates of 33 mol % $2C_{14}Br$/67 mol % CTAB were evaluated to be large and rodlike particles with diameters of 600–1600 Å from electron microscopic and dynamic light-scattering results and that remarkably high enantioselectivity (L/D = 71) was obtained at this specific coaggregate composition. (d) On the basis of the CD experiments, the active tripeptide (Z-PheHisLeu) has a possibility to constitute a hydrophobic pocket through the intramolecular interactions between the side chains of the Phe, His, and Leu residues. As regards the remarkably high enantioselectivity, it is suggested that the adjusting of the hydrophobic microenvironment to the optimum fit of Z-PheHisLeu and L-S_{12} by changing the composition of coaggregates could be a very important factor along with the favorable fitting of reactants as demonstrated in the CPK model.

It is very important that stereochemical control of the enantioselective hydrolysis of amino acid esters could be established by temperature regulation and by changing the composition of the coaggregates (reaction field). The stereoselectivity was optimized at temperatures somewhat higher than the aggregate phase transitions and on the verge of phase separation, the so-called boundary regions. This distinctive behavior might be related to the activation of native enzymes at the boundary between stable and unstable regions (pH, temperature, and so on).

Acknowledgment. We thank Dr. Toshihiko Takaki (Kyushu University) for his technical assistance in electron microscopy and Toshiro Nagamatsu and Takashige Yoshino (Kumamoto Institute of Technology) for their technical assistance in kinetic measurements. This work was supported in part by a Grant-in-Aid for Scientific Research from the Ministry of Education, Science, and Culture of Japan (No. 61550648); at Rutgers University, we acknowledge support by the U.S. Army Research Office.

Registry No. D-**1a**, 14009-95-1; L-**1a**, 14009-94-0; D-**1b**, 75531-12-3; L-**1b**, 75531-11-2; D-**1c**, 2578-85-0; L-**1c**, 2578-84-9; **2a**, 14997-58-1; **2b**, 16804-63-0; **3a**, 38972-90-6; **3b**, 89092-59-1; **3c**, 13053-69-5; **4a**, 79778-48-6; **4b**, 20806-38-6; **5**, 31373-65-6; **6**, 28458-19-7; **7a**, 68105-02-2; **7b**, 70755-47-4; **7c**, 1812-53-9; **8a**, 57-09-0; **8b**, 112-02-7; Cbz-D-Phe-OH, 2448-45-5; Cbz-L-Phe-OH, 1161-13-3; H-L-His-OH, 71-00-1; H-L-His-L-Leu-OH, 7763-65-7; $H_3C(CH_2)_{12}COCl$, 112-64-1; $H_3C(CH_2)_{13}NMe_2$, 112-75-4; $H_3C(CH_2)_{15}NMe_2$, 112-69-6; $H_3C(CH_2)_{13}Br$, 112-71-0; $H_3C(CH_2)_{15}Br$, 112-82-3; $H_3C(CH_2)_{15}Cl$, 4860-03-1.

(28) Harada, N.; Nakanishi, K. *Circular Dichroic Spectroscopy Excition Coupling in Organic and Bioorganic Chemistry*; University Science Books: Mill Valley, CA, 1983.
(29) (a) Holzwarth, G.; Doty, P. *J. Am. Chem. Soc.* **1965**, *87*, 218. (b) Chen, Y.-H.; Yang, J. T.; Chau, K. H. *Biochemistry* **1974**, *13*, 3350. (c) Higashijima, T.; Wakamatsu, K.; Takemitsu, M.; Fujino, M.; Nakajima, T.; Miyazawa, T. *FEBS Lett.* **1983**, *152*, 227.
(30) Steitz, T. A.; Henderson, R.; Blow, D. M. *J. Mol. Biol.* **1969**, *46*, 337.
(31) Murakami, Y.; Nakano, A.; Matsumoto, K.; Iwamoto, K. *Bull. Chem. Soc. Jpn.* **1978**, *51*, 2690.